Supplementary Materials for

Bacterial Vesicles in Marine Ecosystems

Steven J. Biller,* Florence Schubotz, Sara E. Roggensack, Anne W. Thompson, Roger E. Summons, Sallie W. Chisholm*

*Corresponding author. E-mail: chisholm@mit.edu (S.W.C.); sbiller@mit.edu (S.J.B.)

Published 10 January 2014, *Science* **343**, 183 (2014)
DOI: 10.1126/science.1243457

This PDF file includes

Materials and Methods
Supplementary Text
Figs. S1 and S13
Tables S1 to S6
References

Materials and Methods

Culture conditions
Cyanobacteria were cultured in Pro99 media (*31*) prepared with 0.2 μm filtered, autoclaved seawater collected from Vineyard Sound, MA. Cells were grown under constant light flux (30 – 40 μmol Q m^{-2} s^{-1} for axenic strain MED4; 10 – 20 μmol Q m^{-2} s^{-1} for axenic strains MIT9313, NATL2A and WH8102) at 21 °C, in acid-washed glassware. Media for larger (2 - 20L) cultures was supplemented with 10 mM (final concentration) filter-sterilized sodium bicarbonate upon inoculation, and cultures were grown with gentle stirring (60 rpm).

Vesicle purification
Large quantities of vesicles for biochemical analysis or experimentation were collected as follows (adapted from (*32*)). 2 - 20 L *Prochlorococcus* cultures were grown to mid / late exponential growth phase and gently gravity filtered through a 0.2 μm capsule filter (Polycap 150TC; Whatman). The filtrate was then concentrated using a tangential flow filter (Pall Ultrasette; Omega membrane, 100 kDa cutoff) connected to a Masterflex peristaltic pump (Cole-Parmer); feed pressure was kept < 10 psi throughout processing. Culture volume was reduced to ~40 mL, recirculated through the filter for 10 minutes to recover material from the membrane, and then eluted. This concentrated supernatant was gently filtered through a 0.2 μm syringe filter (Pall, Supor membrane) to ensure that no cells remained, and pelleted by ultracentrifugation at ~100,000 x*g* (Beckman-coulter SW32Ti rotor; 32,000 rpm, 2 hrs, 4 °C).

Vesicles were purified from other material in the cultures using an Optiprep (Iodixanol; Sigma-Aldrich) density gradient as follows. The vesicle pellet was first resuspended in 0.5 mL of 45% Optiprep in a buffer containing 3.6% (w/v) NaCl (to maintain seawater salinity) and 10 mM HEPES, pH 8. This was placed in the bottom of a 4 mL UltraClear ultracentrifuge tube (Beckman Coulter) and overlaid with equal volumes of 40%, 35%, 30%, 25%, 20%, 15%, 10% and 0% Optiprep (in the same buffer background). The gradient was centrifuged at 100,000 x *g* (32,000 rpm) for 6 hours at 4 °C in a SW60Ti rotor (Beckman Coulter), and 0.5 mL fractions collected. Material in each fraction was recovered by diluting the sample at least 5-fold with buffer (10 mM HEPES / 3.6% NaCl) and pelleting in an ultracentrifuge (~100,000 x *g*, 1 hr, 4 °C, SW60Ti rotor). Vesicles typically migrated to Optiprep densities between 1.14 – 1.19 g/mL; vesicles from *Prochlorococcus* cultures were typically found in the range of 1.14 – 1.17 g/mL, and vesicles from field samples were found between 1.15 – 1.19 g/mL. This final pellet was resuspended in fresh buffer and frozen at -80 °C. Electron microscopy was routinely used to confirm the contents and purity of vesicle fractions (see below).

Field sampling of vesicle content was conducted as follows. Water was collected into 25 L carboys (~100 L total coastal surface water from Vineyard Sound, MA: 41° 31.42’ N, 70° 40.32’ W, collected in September 2012; ~280 L total from each depth sampled at the Bermuda Atlantic Time-series station: 31° 39.96’ N, 64° 9.84’ W, collected in December 2012). Samples were processed within two hours of collection. This water was slowly pumped through a 0.2 μm capsule filter (Polycap 150TC; Whatman) and concentrated using a Centramate tangential flow filter equipped with five 100 kDa Omega filter modules (Pall); the final concentrate was frozen at -80 °C. This concentrate was later thawed, pelleted as above, and the pelleted material purified

across an Optiprep density gradient (also as above, except the gradient was run for 6 hours at 45,000 rpm and 0.4 mL fractions collected).

Vesicle quantitation
Vesicle concentrations were measured by nanoparticle tracking analysis using a NanoSight LM10HS instrument (NanoSight Ltd, UK), equipped with a blue laser module and NTA software V2.3. Samples were diluted such that the average number of particles per field was between 20-60, per the manufacturer's guidelines. Two to three replicate videos were collected from each sample (by pushing additional sample through the chamber in order to acquire a different field), and analyzed as technical replicates. The sample chamber was thoroughly flushed with 18.2 $M\Omega\ cm^{-1}$ water (Milli-Q; Millipore) between samples, and visually examined to ensure that no particles were carried over between samples. All data files for a given experiment were processed using identical settings (typical setting range: camera shutter 30-45ms; camera gain 300-400; detection threshold 5-7; auto blur). The vesicle concentration in the sample was defined based on the measurement of total particles between 50 - 250 nm diameter.

Vesicle concentrations from field samples were estimated based on the total number of particles in the most vesicle-enriched gradient fraction (as assessed visually by electron microscopy), normalized to the total amount of water originally concentrated for that sample. Thin filamentous features of these fractions, visible by electron microscopy, were below the detection limit of the NanoSight. We note that our field concentration measurements represent minimum estimates, as we do not consider vesicles present in other gradient fractions besides the maximal one. This approach was intentionally conservative and designed to minimize the potential impact of counting any non-vesicle particles in the enriched field samples.

Vesicle stability analysis
Three replicate 40 mL axenic *Prochlorococcus* MED4 cultures were grown to mid-exponential phase as described above. Cultures were filter sterilized through a 0.2 μm Supor syringe filter (Pall) and placed in a 21 °C incubator. 1 mL samples were collected every two days and frozen at -20 °C. The concentration and mode diameter of the vesicles (again, defined as particles between 50 - 250 nm diameter) were measured using the NanoSight as described above.

Vesicle production measurements
To measure vesicle concentrations in growing cultures, triplicate 40 mL axenic *Prochlorococcus* cultures were grown as described above in *Culture conditions*. Daily 1mL samples were collected and fixed for flow cyometry analysis with 0.125% (final concentration) glutaraldehyde for 10 minutes in the dark; samples were then flash frozen in liquid nitrogen and stored at -80 °C until they were analyzed. For vesicle samples, 1 mL of culture was gently filtered through a 0.22 μm syringe filter (Pall, Supor membrane) to separate vesicles from the cells; the filtrate was frozen at -80 °C until analysis. *Prochlorococcus* concentrations in each sample were measured using an Influx flow sorter (BD/Cytopeia) and FlowJo software (TreeStar). Vesicle samples were examined by nanoparticle tracking analysis as described above under *Vesicle quantitation*.

Electron microscopy
For scanning electron microscopy, 2 mL samples of *Prochlorococcus* culture were first fixed with 2% glutaraldehyde in solution for 15 minutes at room temperature in the dark, and then

gently pushed onto a 0.1 μm Supor filter (Pall) using a syringe and Swinnex filter holder (Millipore). Cells on the filter were further fixed in a 2% glutaraldehyde / 3% paraformaldehyde / 5% sucrose solution in a sodium cacodylate buffer (pH 7.4) for 1 hour at room temperature. The filter was washed with 0.1 M phosphate buffer, and then treated with 1% osmium tetroxide for 1 hour at room temperature. The filter was again washed in 0.1M phosphate, then dehydrated using an ethanol gradient (50%, 75%, 95%, 100%, 100% ethanol; 15 minutes each). Next, the cells on filter paper were critical point dried, and sputter coated before imaging on a JEOL 6320FV scanning electron microscope.

For negative stain TEM images, 5 μL of vesicle sample was applied to a freshly charged Formvar-coated copper grid (Electron Microscopy Sciences) for 5 minutes. The grid was then briefly washed with 1 mM EDTA (pH 8), stained with 2% uranyl acetate for 1 minute, and allowed to dry. Grids were imaged on a JEOL JEM-1200ex II transmission electron microscope at 60KV with an Advanced Microscopy Techniques (AMT) camera.

For thin section TEM images, the material was fixed in 2.5% gluteraldehyde, 3% paraformaldehyde with 5% sucrose in 0.1M sodium cacodylate buffer (pH 7.4) for one hour at room temperature. The samples were pelleted and post fixed in 1% OsO_4 in veronal-acetate buffer. The pellet was stained in block overnight with 0.5% uranyl acetate in veronal-acetate buffer (pH 6.0), then dehydrated and embedded in Embed-812 resin. Ultra-thin sections were cut on a Reichert Ultracut E microtome with a Diatome diamond knife, and stained with uranyl acetate and lead citrate. The sections were examined using a FEI Tecnai spirit at 80KV and photographed with an AMT camera.

Lipid characterization

10 L cultures of axenic *Prochlorococcus* strain MED4 or MIT9313 were grown as described above to late exponential phase. 50 mL samples were collected into cleaned and fired glass tubes for whole cell analysis. Vesicles were isolated by TFF and gradient purified as described above and washed twice in 10 mM HEPES pH 8 / 3.6% NaCl buffer. Contents and purity of the fractions were verified by TEM.

Lipids were extracted with a modified Bligh and Dyer protocol (after (*33*)) and analyzed by high-performance liquid chromatography-mass spectrometry (HPLC-MS) following methods previously established (*34*). Here, glyco- and phospholipids were separated on a Waters Acquity UPLC BEH Amide column (125 mm x 2mm, 5μm) with a linear solvent gradient on a Agilent 1200 series HPLC system coupled to an Agilent 6520 accurate-mass quadrupole time-of-flight MS with an electrospray ionization interface (ESI). Quantification of glyco- and phospholipids was accomplished by comparison of peak area counts. Response factor were accounted for by verification of relative peak areas of known amounts of authentic standards (Avanti Polar Lipids, USA; Lipid Products Redhill, UK). An aliquot of the total lipid extract was acid hydrolyzed to produce fatty acid methyl esters (FAMEs) by treatment with methanolic HCl at 100°C (3 h). FAMEs were identified and quantified with a Varian CP-Sil-5 fused silica capillary column (60 m x 0.32 mm, 0.25 um) using an Agilent 7890 gas chromatograph coupled to an Agilent 5975C mass-selective detector.

Endotoxin measurements
The presence of Lipid A (endotoxin) in purified vesicle samples was determined using the LAL Chromogenic endotoxin quantitation kit (Pierce) following the manufacturer's instructions. Vesicle samples were positive for endotoxin, with signal significantly (>6-fold) above buffer background measurements.

Measuring vesicle protein content
Protein content of vesicle samples was determined using the Micro BCA Protein Assay Kit (Pierce), following the manufacturer's directions for the microplate assay. Vesicle samples were washed and resuspended in 1X PBS for this measurement.

Vesicle proteomics analysis
Vesicles were isolated from 20L axenic *Prochlorococcus* cultures and gradient purified as described above, then washed three times in 1X PBS. The sample was mixed with SDS-PAGE sample buffer (60mM Tris-HCl pH 6.8, 8% glycerol, 1% SDS, 1% 2-Mercaptoethanol and 0.005% bromophenol blue) and incubated at 95 °C for 5 minutes. Proteins were run out on an AnykD SDS-PAGE gel (Bio-Rad), which was stained with the Bio-Rad Silver Stain Plus kit following the manufacturer's instruction. Mass spectrometry analysis was carried out at the MIT Koch Institute Swanson Biotechnology Center proteomics core. Briefly, gel slices from the entire band were removed from the gel, destained, reduced with dithiothreitol, alkylated with iodacetamide and digested with trypsin. LC-MS analysis of the digested peptides was carried out on a LTQ mass spectrometer (Thermo Fisher), and searched against protein databases with Mascot (Matrix Science). Identification probability was assigned by Mascot; we required each identified protein to have at least one exclusive unique peptide and a protein identification probability >97%. The subcellular localization for each protein is based on predictions from PSORTb (*35*).

Vesicle-associated DNA purification and sequencing
Gradient-purified vesicle fractions (from both culture and field samples) were pelleted by ultracentrifugation (100,000 xg, 1 hr, 4 °C, SW60Ti rotor) and washed three times in sterile 1X PBS; the final pellet was resuspended in 100 μL PBS. To eliminate any DNA remaining in the sample outside of the vesicles, samples were first treated with 2U of TURBO DNase (Invitrogen) according to the manufacturer's instructions in a 50 μL final reaction volume and incubated for 30 minutes at 37 °C. Following this, an additional 2U of TURBO DNase enzyme was added and incubated as before. DNase was inactivated at 75 °C for 15 min. Genomic DNA controls were used to confirm the effectiveness of the DNase treatment.

To lyse the vesicles, samples were incubated in GES lysis buffer (*36*) (50 mM guanidinium thiocyanate, 1 mM EDTA, and 0.005% (w/v) sarkosyl; final concentration) at 37 °C for 30 minutes. DNA was purified using DNA Clean & Concentrator-5 columns (Zymo Research) per the manufacturer's instructions, using a 5:1 ratio of DNA binding buffer, and eluted in ultrapure water. DNA content of samples was measured by the Quant-iT PicoGreen dsDNA assay (Invitrogen) or by an Agilent Bioanalyzer High Sensitivity DNA assay, per the manufacturer's directions.

RNA was isolated as above, except the DNase treatment was carried out after lysis, not before. RNA was purified from the sample using RNAClean XP beads (Beckman-Coulter) following the

manufacturer's protocols. RNA content was measured using Quant-iT RiboGreen assay (Invitrogen), per the manufacturer's directions. RNA sequencing libraries were constructed as in (*37*); one library was constructed without any rRNA depletion steps and sequenced on an Illumina MiSeq (150+150nt paired reads), and the other used a duplex-specific nuclease approach to remove rRNA and achieve a higher sequencing depth (*37*), and was sequenced on an Illumina HiSeq (40+40nt paired reads).

To obtain sufficient DNA for sequencing library construction, samples of purified vesicle DNA were amplified by multiple displacement amplification (MDA) using the RepliPHI Phi29 polymerase (Epicentre) in 20 μL reactions following the manufacturer's protocols with the following modifications: all plasticware, water and buffers were thoroughly UV treated in a Stratalinker (Stratagene), as was the final reaction master mix (1hr) (*38*). 0.2x (final concentration) SYBR Green I (Invitrogen) was added to the master mix following UV treatment. The reaction was incubated at 30 °C for 10 hours in a LightCycler (Roche), monitoring the SYBR signal to confirm whether reactions worked. For each sample, three independent amplification reactions were pooled to minimize some sources of amplification bias, and purified using the Qiagen QiaAmp DNA mini kit (following the supplementary protocol for "Purification of REPLI-g amplified DNA"). Sequencing libraries were constructed from this MDA-amplified sample as previously described (*39*), except we used a double SPRI bead ratio of 0.65/0.15 to purify fragments with an average size of ~340 bp (range: 200-600 bp). DNA libraries were sequenced on an Illumina MiSeq, yielding either 150+150nt or 250+250nt paired reads, at the MIT BioMicro Center.

Sequence analysis

Low quality sequence regions were removed from the raw Illumina data using quality_trim (from the CLC Assembly Cell package, CLC bio) with default settings. Alignment of vesicle DNA sequences from cultured *Prochlorococcus* samples to the appropriate reference genome was done with the Burrows-Wheeler Aligner (*40*), and resultant alignment files parsed with aid of the samtools package (*41*). An ORF was considered to be present in the RNAseq data if there were at least 10 reads that mapped within the gene boundaries.

To examine the content of vesicle DNA from field samples, MiSeq reads were overlapped using the SHE-RA algorithm (*42*), keeping any reads with an overlap score > 0.5; reads that did not successfully overlap were included as well. Reads were searched against the NCBI nr protein database (March 15, 2013 release) using UBLAST (*43*) with the following parameters: "-evalue 1-e9 -weak_evalue 0.001 -maxhits 1 -blast6out". Hits having an e-value > 1e-4 or a bitscore < 50 were removed, and only the top hit was retained.

From the coastal sample, 344,420 sequences out of 2,417,029 original paired sequence reads (14.2%) had significant homology to a sequence in the nr database at this threshold; 80,487 out of 1,632,832 (4.9%) original paired reads from the open ocean vesicle library had significant homology. NCBI taxonomy classification from the top nr hit was used to assign a putative origin for each unique sequence. Because the vesicle DNA used for library construction was MDA amplified and thus subject to great amplification bias, especially toward overamplifying ssDNA viruses (*44*), we report on the number of unique sequences in the nr database matched by library

reads. This metric provides a qualitative description of the diversity present in the samples, and we do not draw any detailed quantitative conclusions about relative abundance from these data.

Heterotroph growth assays

The heterotroph strains tested were previously isolated from cultures of *Prochlorococcus* strain MED4 and MIT9313 (S. Bertilsson, unpublished) and are available upon request. Heterotrophs were grown at room temperature in a medium made from 0.2 μm filtered and autoclaved seawater, supplemented with 800 μM NH_4Cl, 50 μM NaH_2PO_4, 1X Pro99 trace metal mix, 1x Va vitamin mix, and 0.05% (w/v) each sodium pyruvate, sodium acetate, sodium lactate, and glycerol (ProMM) (*45*). Stationary phase heterotroph cultures were washed three times in Pro99 media made from 0.2 μm filtered and autoclaved Sargasso seawater (centrifuging for 5 min at 16,000 x*g*) and diluted to an identical starting OD_{600} to begin the growth assay.

Purified vesicles (or, as a control, samples of sterile Pro99 media put through the identical vesicle purification process) were washed three times in Pro99 media by ultracentrifugation as above. Vesicle samples, the media control, or a defined mixture of organic carbon compounds (sodium pyruvate, sodium acetate, sodium lactate, and glycerol; final concentration 0.001% (w/v) each) were added to replicate wells. Cells were grown in 96-well plates, and growth was measured by following the OD_{600} on a Synergy 2 plate reader (BioTek) at 27 °C, measuring optical density every hour for 48 hours. To confirm that the change in OD_{600} corresponded to an increase in cell abundance within the culture, dilutions of culture samples from the beginning and end of the timecourse were plated on ProMM plates containing 1.5% agar. Plates were grown at room temperature and the number of colony forming units counted (n=3 replicates).

Examining vesicle-phage interactions

Samples of cyanophage PHM-2 were inoculated into exponentially-growing cultures of *Prochlorococcus* strain MED4. Once the infected culture had visibly lysed (typically 3-5 days), the culture was put through a 0.2 μm Supor filter (Pall) and phage were precipitated by ultracentrifugation (Beckman SW32Ti rotor, 32,000 rpm, 4°C, 1hr) and resuspended in 100 μL of fresh Pro99 media. 10 μL of phage were mixed with an equal volume of purified MED4 vesicles, incubated for 15 min at room temperature, and examined by negative stain electron microscopy as above.

Supplementary text

Description of vesicle carbon content estimates

We base our estimates of average vesicle carbon content on the carbon from lipids only, as the distribution of other organic compounds within vesicles (e.g. DNA, RNA, protein) is not necessarily uniform; thus this is a lower-bound estimate of carbon content. We assume that vesicles are spherical, with a diameter of 75 nm (the average mode abundance in our field samples, fig. S9A), and are enclosed by a single lipid bilayer. We then calculate the total number of lipid molecules per vesicle based on the total surface area of the vesicle, assuming an average area of 0.54 nm^2 per lipid molecule (*46*) and that lipids make up a total of 80% of the membrane area (*47*). Total carbon content is then derived from the number of lipid molecules and an average of 43 C atoms per lipid molecule, based on the measured abundance of different lipid species in *Prochlorococcus* vesicles (fig. S5). The minimum carbon content for a 75 nm diameter vesicle is ~0.05 fg C, but varies from 0.02 fg to 0.3 fg C for vesicles of 50 nm and 200 nm diameter, respectively. As an average bacterial cell in the open ocean contains ~12 fg carbon (*48*), a single vesicle could contain, on an order-of-magnitude basis, $1/100^{th}$ the carbon of a heterotroph.

Calculating vesicle production per cell per generation

Measured vesicle production by *Prochlorococcus* cultures during exponential growth is consistent with a model wherein, on average, each cell releases a constant number of vesicles per generation, as described below. We also assume that vesicle loss in the culture is negligible, as we have shown that they are stable in seawater for at least two weeks (fig. S4).

The number of vesicles (V) produced by a population of cells during the time it takes the population to double (i.e. one generation time) is thus the product of the total number of cells (N) in the population and r, the average number of vesicles released per cell per generation:

$$V = Nr \tag{1}$$

More generally, given the initial number of cells in the population (N_0), the number of vesicles produced in the xth generation (V_x) is:

$$V_x = 2^{x-1} N_0 r \tag{2}$$

The total number of vesicles (V_{total}) in the culture after n generations is then:

$$V_{total} = \sum_{x=1}^{n} 2^{x-1} N_0 r = (2^n - 1) N_0 r \tag{3}$$

For each culture, we determine the instantaneous growth rate, μ ($time^{-1}$), for the *Prochlorococcus* cells during exponential growth (from time a to b) from the number of cells, N_a and N_b, respectively, present at the beginning and end of the log-linear portion of the growth curve:

$$\mu = \frac{\ln\left(\frac{N_b}{N_a}\right)}{(b-a)} \quad (4)$$

which allows us to calculate the number of generations (n) per unit time as:

$$n = \frac{\mu(b-a)}{\ln(2)} \quad (5)$$

To determine the number of vesicles produced per cell per generation in our culture, we solve for r (in Eq. 3 above) in terms of the number of vesicles produced during exponential growth, and the number of generations that occurred during this timespan:

$$r = \frac{V_{total}}{N_0(2^n - 1)} = \frac{V_b - V_a}{N_0(e^{\mu(b-a)} - 1)} \quad (6)$$

where V_a and V_b represent the number of vesicles measured at the beginning and end of exponential phase, respectively. This model fit the observed vesicle production during exponential growth for the three strains examined well, with correlation coefficients between modeled and observed concentrations of 0.89 (MED4), 0.95 (NATL2A) and 0.96 (MIT9313) (fig. S13 and Table S1).

Estimates of global Prochlorococcus *vesicle production*

We calculated an order-of-magnitude estimate of global *Prochlorococcus* vesicle production as follows. Our data from cultured *Prochlorococcus* strains, representing multiple ecotype groups, is consistent with the assumption that most or all *Prochlorococcus* cells release vesicles. In the field, the generation time of *Prochlorococcus* is between 1 - 2 days (*49*, *50*); given a mean global *Prochlorococcus* abundance of ~3 x 10^{27} cells (*14*), this implies that on the order of 1.5 x10^{27} – 3 x10^{27} new *Prochlorococcus* cells are produced per day. The *Prochlorococcus* cultures examined in this study grew with a similar generation time as has been shown for cells in the oceans (*49*, *50*), and released 2 - 5 vesicles per cell per generation (see above). While environmental factors may influence *Prochlorococcus* vesicle release in the field relative to those in observed in culture, based on these numbers we estimate that global *Prochlorococcus* populations could release ~10^{27} – 10^{28} vesicles per day. Since *Prochlorococcus* vesicles contain, conservatively, on the order of 0.05 - 0.1 fg carbon each, global C release in the form of *Prochlorococcus* vesicles would then be ca. 10^4 – 10^5 tonnes C per day.

Vesicle-associated lipids in field samples

The distribution of intact polar lipid headgroups from vesicle-enriched field samples (fig. S10) was notably different from that seen in cultured *Prochlorococcus* strains (fig. S5). This result is consistent with the hypothesis that many marine microbes besides cyanobacteria release vesicles, which is also supported by the presence of DNA from diverse organisms within this sample (Table S5).

The presence of monoglycosyldiacylglycerol is consistent with phototroph-derived vesicles, as this is typically the dominant lipid in their thylakoid and cytoplasmic membranes (*51*), although other cyanobacterial lipids such as sulfoquinovosyldiacylglycerol were not detected in these field samples. While betaine lipids and phosphotidylcholine are typically thought to originate from algae and would suggest an algal origin for many of these vesicles (some algal species were identified by DNA sequencing; Table S5), fatty acid analysis identified primarily saturated $C_{14:0}$ and $C_{16:0}$ species in these samples. Since algal fatty acids are dominantly polyunsaturated (*52*), this implies that much of the betaine and phosphotidylcholine in vesicles may in fact be of bacterial origin (*53*). This conclusion finds additional support in the recent identification of abundant betaine lipids in Proteobacteria (*54*) and in bacterial biofilms that coat Bahamian ooid sand grains (*55*). Although we were somewhat surprised to not find common heterotrophic phospholipids such as phosphotidylethanolamine, given the relative abundance of Proteobacterial sequences in the data set, phosphatidyldiacylglycerol can also be derived from heterotrophs (*56*).

Phage content of enriched vesicle fraction sequencing libraries

While bacterial sequences comprised the majority of unique database hits recovered (Table S5), we also identified reads with significant homology to phage sequences (largely capsid and replication proteins) within both the coastal and open ocean data sets (8% of total coastal reads, 4% of total open ocean reads). The presence of phage DNA among the sequences in our vesicle preparations could result from several sources: (i) Phage co-isolated with the vesicles in the density gradient fraction; (ii) Phage genomes that have been injected into vesicles through mistaken infection; or (iii) Phage sequences packaged in vesicles as prophage (see Fig. 4).

Some phage, such as the tailed phage known to infect cyanobacteria, are known to incorporate host-like genes in their genomes (*57-61*). The presence of host-like genes in vesicle-associated phage genomes could introduce some ambiguity to our conclusion that most bacterial genes found in the vesicle samples have their origins in DNA exported by microbes within vesicles. Though a few of the bacterial sequences we found in the vesicles could possibly have come from phage, this is not likely to account for a significant portion of the genes identified for the following reasons:

First, the ssDNA phage (*Circoviridae*, *Geminiviridae*, *Microviridae*, *Nanoviridae*) sequences, which account for a large portion of the phage reads, almost certainly result from co-isolation of these phage with the vesicles, as what appear to be ssDNA filamentous phage are visible in electron micrographs of our vesicle fractions (see Fig. 3A-B). We note that ssDNA phage are also known to be preferentially enriched by multiple displacement amplification (*44*), which may have resulted in a relative oversampling of these sequences. These phage have small (< 12kb) genomes (*62*, *63*) and typically do not carry genes of host origin. Second, the read abundance distributions of bacterial and phage genes in the dataset were significantly different (Mann-Whitney test, $p < 2.2 \times 10^{-16}$ in both libraries), demonstrating that, on the whole, they did not originate from the same DNA molecules. Finally, paired-end data do not show clear examples where bacterial and phage genes were found on the same DNA fragment (Additional data table S6). We examined the nonoverlapping (and thus presumably longest, from >450 bp fragments) paired-end sequences, finding that only 4.6% of the 38,822 reads in the coastal sample with significant BLASTx hits on both ends matched a phage protein on one end and a bacterial protein on the other (only 0.5% of paired reads differed in the open ocean sample). Of these

mixed sequence pairs, the putative bacterial sequence was nearly always one of two hypothetical proteins (NCBI gi 423339592 and 15618146); these sequences each have significant similarity to other phage genes, and we suspect they may have been mis-annotated.

For all of these reasons, we argue that the vast diversity of microbial sequences isolated from the enriched vesicle fractions have their origins in DNA exported by microbes within vesicles, and not in phage genomes.

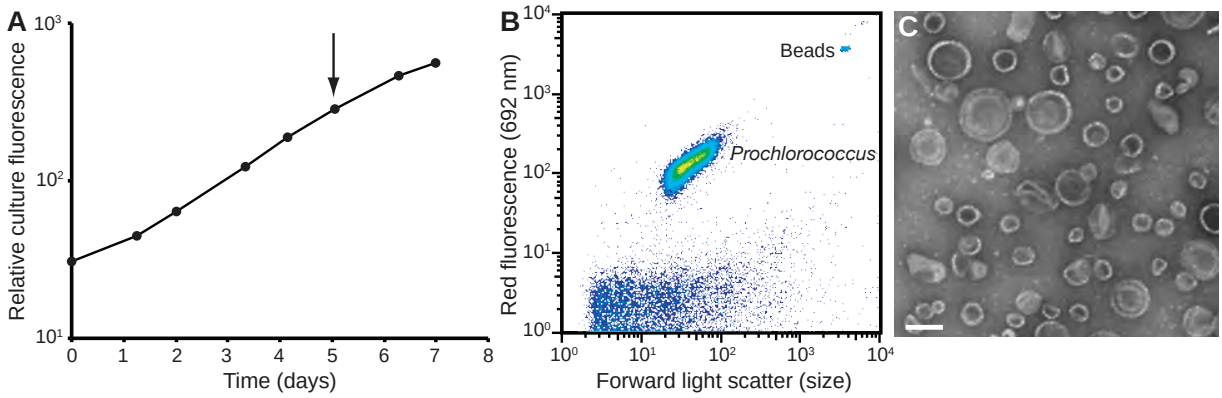

Fig. S1. Vesicles are released by intact, healthy *Prochlorococcus* cells. (**A**) Growth curve of axenic *Prochlorococcus* strain MED4 as measured by relative culture autofluorescence. Vesicles were collected at the timepoint indicated by the arrow, in late exponential growth phase. (**B**) Flow cytometry profile of MED4 cells from the time point indicated in (A), demonstrating a *Prochlorococcus* population distribution indicative of a healthy population. Signals of cells with reduced chlorophyll fluorescence typical of stressed or stationary phase cultures were not observed (signals at red fluorescence values < 10 are instrument noise). 2 µm diameter fluorescent beads (Duke Scientific) were added as an internal size reference. (**C**) Negative stain TEM of vesicles collected from the sample, confirming that vesicles are present in the culture at this time point. Scale bar: 100 nm.

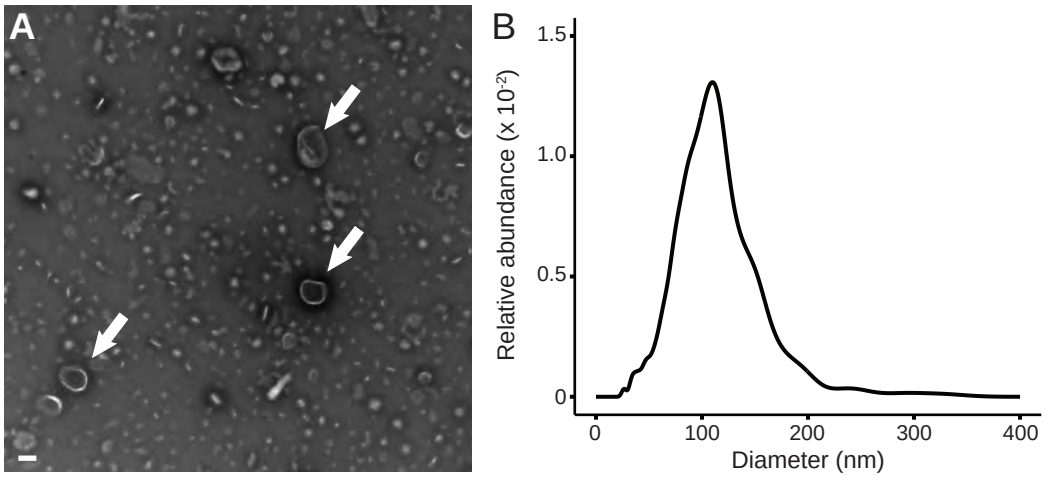

Fig. S2. Vesicles are also released by *Synechococcus* strain WH8102. (**A**) Electron micrograph of vesicles (indicated by arrows) isolated from the supernatant of an exponentially growing culture of axenic WH8102. Material in the background is likely due to a brown compound present in cultures of this strain that co-purified with the vesicles. Scale bar: 100 nm. (**B**) Nanoparticle tracking analysis of WH8102 supernatant indicates that vesicles were present at approximately 1.9 x 10^9 mL^{-1} in culture, with a mode diameter of 110 nm.

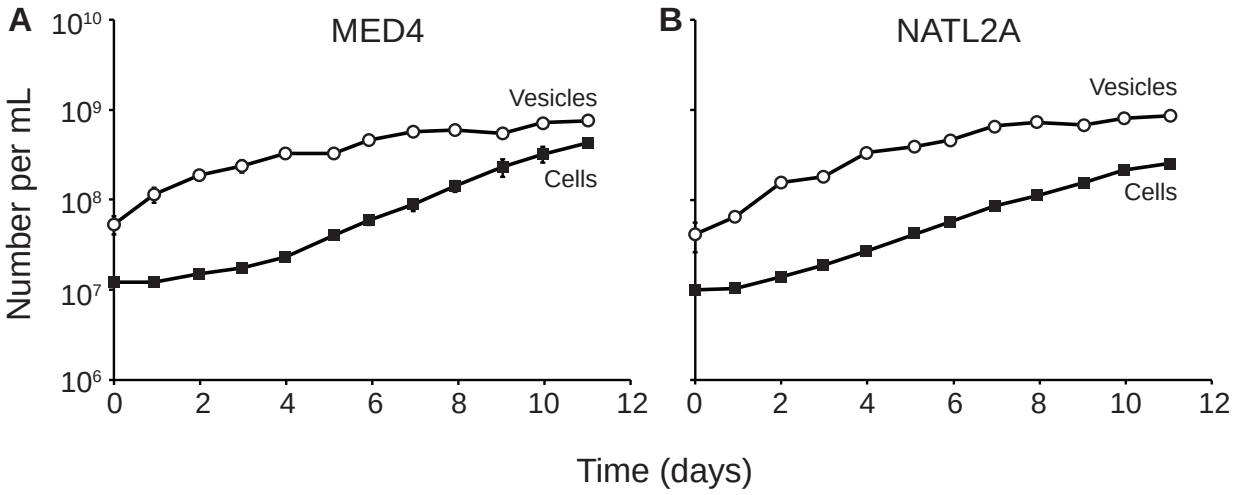

Fig. S3. Vesicle production by different *Prochlorococcus* strains representing two different ecotypes. Vesicle concentration (open circles) as compared to cells (squares) in axenic cultures of *Prochlorococcus* strain (**A**) MED4, a high-light adapted strain, and (**B**) NATL2A, a low-light adapted strain. Cells were grown under constant light as described above, with samples taken daily for measurement of total cells (by flow cytometry) and vesicle concentration (measured using nanoparticle tracking analysis). Values represent the mean +/- SD of three replicates.

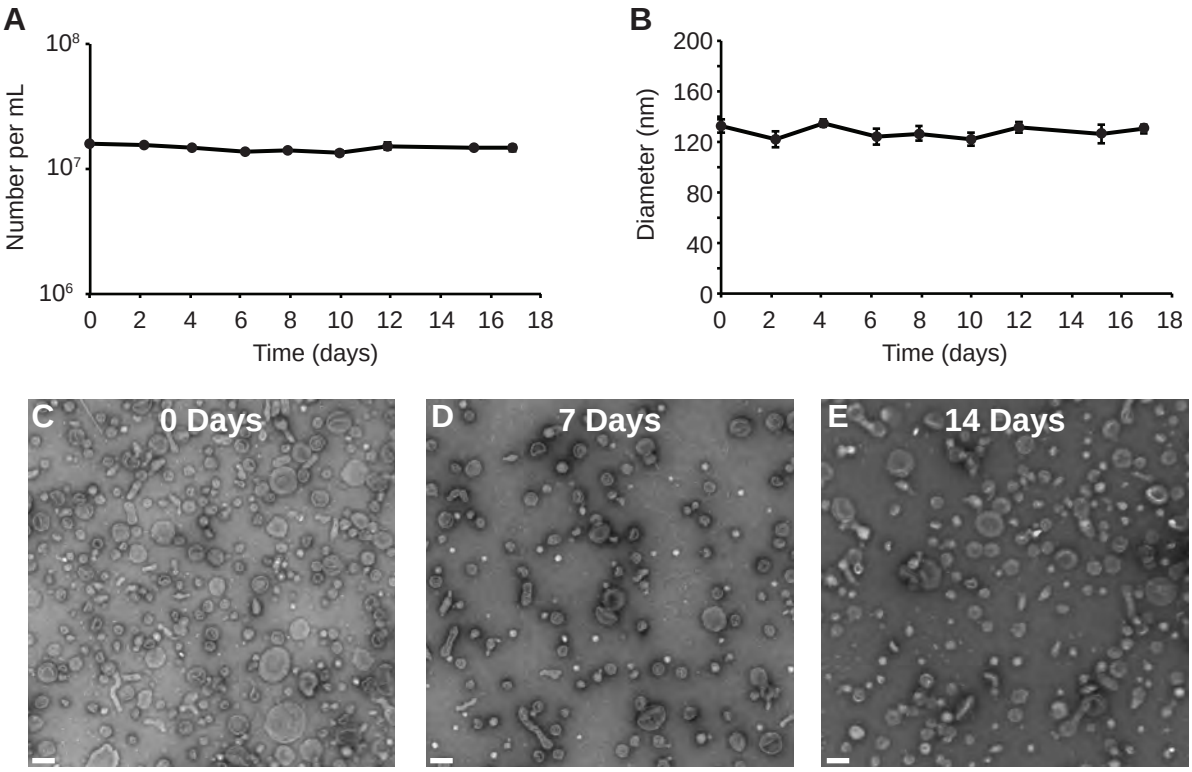

Fig. S4. ***Prochlorococcus*** **vesicles are stable in seawater.** (**A**) The concentration of vesicles in filter-sterilized seawater at 21 °C changed by less than 10% over the span of 17 days. (**B**) Mode vesicle diameter also did not show any significant variation over this 17 day time period. Values in (A) and (B) represent the mean +/- SD of three independent replicates. (**C – E**) Negative stain TEM images indicate the presence of vesicles in seawater after 0, 7 and 14 days, respectively. Vesicles were clearly visible in the sample after two weeks. The electron microscopy protocol was not quantitative, leading to variation in the number of vesicles per microscope field. Scale bars: 100 nm.

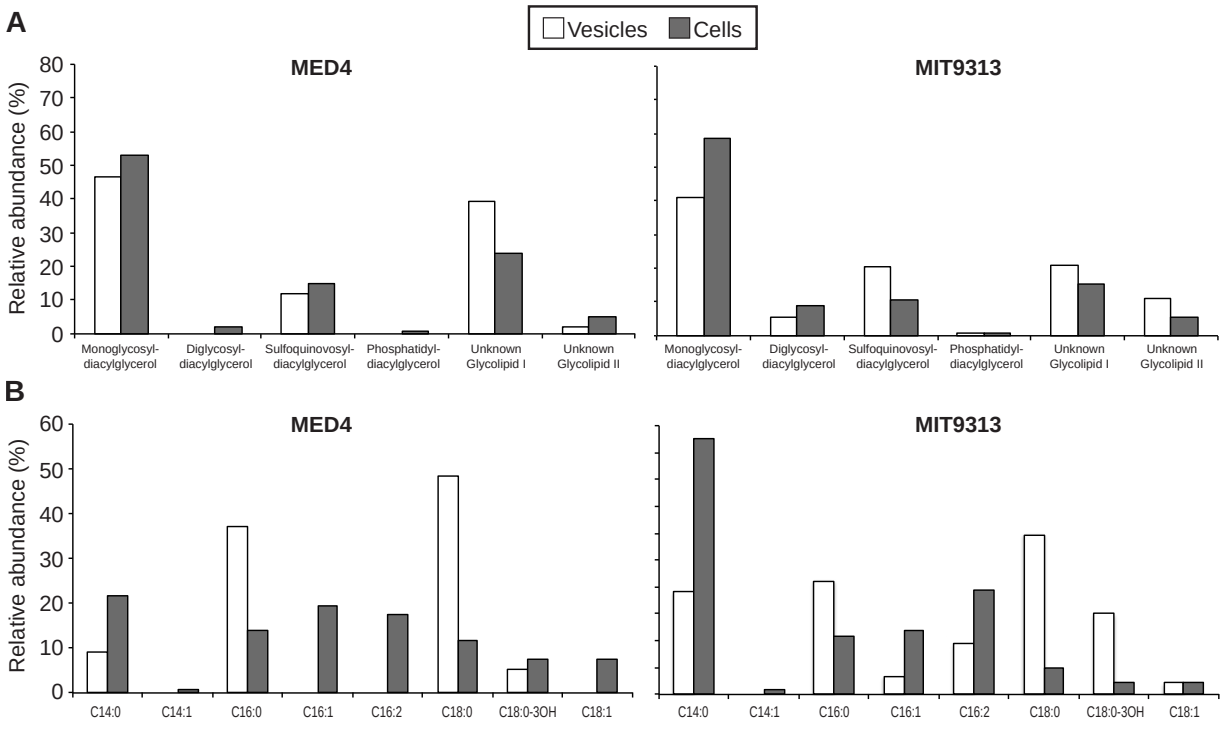

Fig. S5. Lipid characterization of *Prochlorococcus* membrane vesicles. (**A**) Relative abundance of intact polar lipid head groups in MED4 and MIT9313 purified vesicles (white) and cells (grey). Values indicate mean of two biological replicates. (**B**) Relative abundance of polar lipid fatty acids from the same samples.

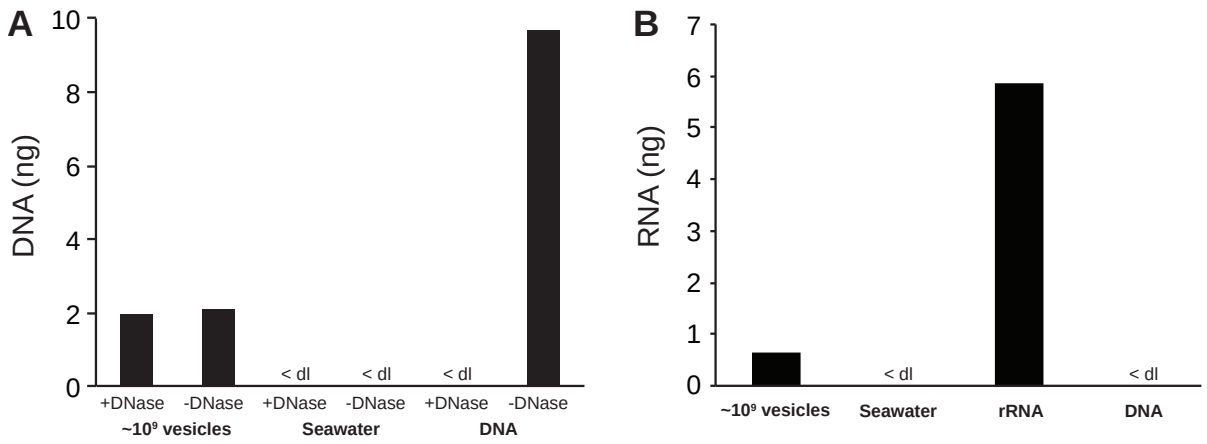

Fig. S6. Quantitation of nucleic acids in purified *Prochlorococcus* vesicles. (**A**) DNA content. Samples of purified *Prochlorococcus* MED4 vesicles, seawater (as a negative control), or *Prochlorococcus* genomic DNA were either treated with Turbo DNase (Ambion) or not, as indicated, prior to lysis, purification and measurement. (**B**) RNA content. Quantitation of RNA obtained from samples of purified *Prochlorococcus* MED4 vesicles or, as controls, seawater, ribosomal RNA, and *Prochlorococcus* genomic DNA. In both plots, '< dl' indicates that concentrations in these samples were below the assay detection limit (~25 pg mL^{-1}). Values represent the mean of two replicate assays.

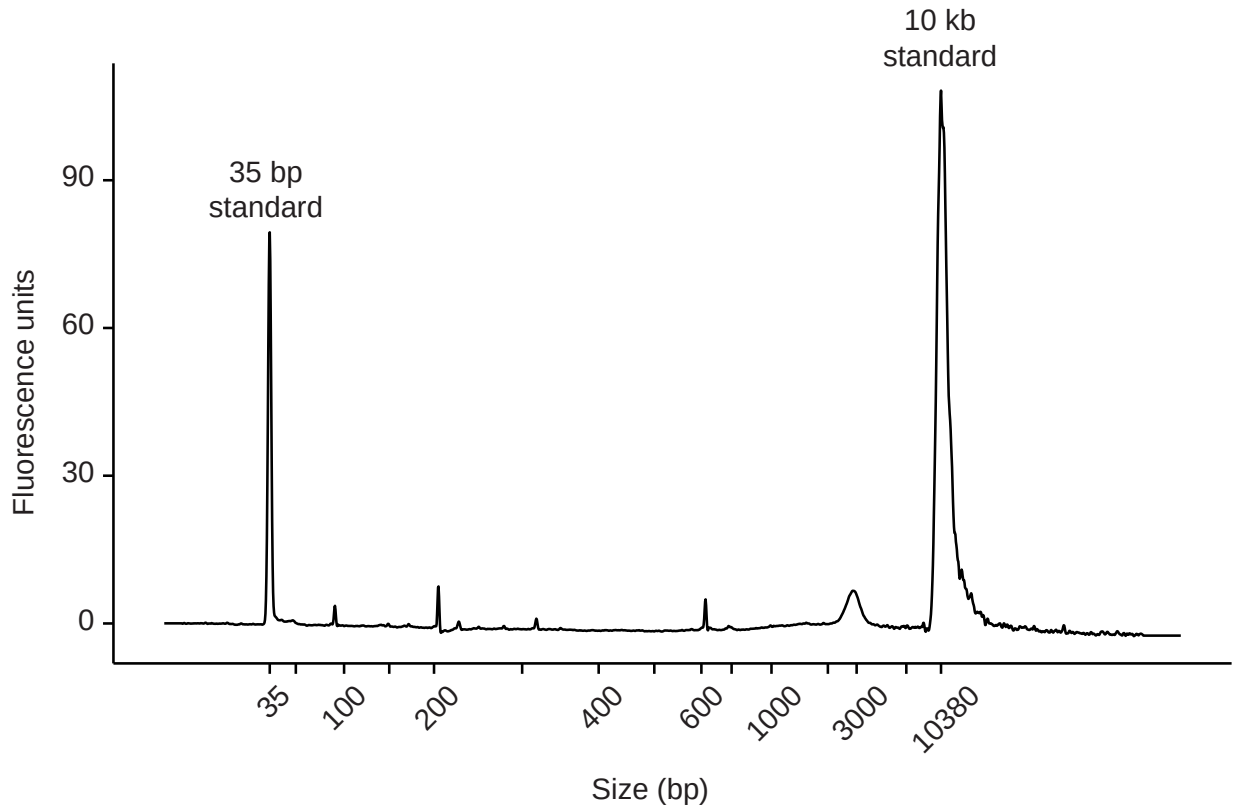

Fig. S7. Size distribution of vesicle DNA fragments from *Prochlorococcus* MED4. Purified vesicle DNA was analyzed with an Agilent BioAnalyzer High Sensitivity DNA assay. Vesicle DNA fragments were found at 92, 206, 318, 612, and 2858 bp. The large peaks at 35 bp and 10380 bp represent internal size standards and not DNA from the sample. This analysis cannot resolve fragments larger than ~7 kb, and we cannot rule out the existence of larger fragments in the sample.

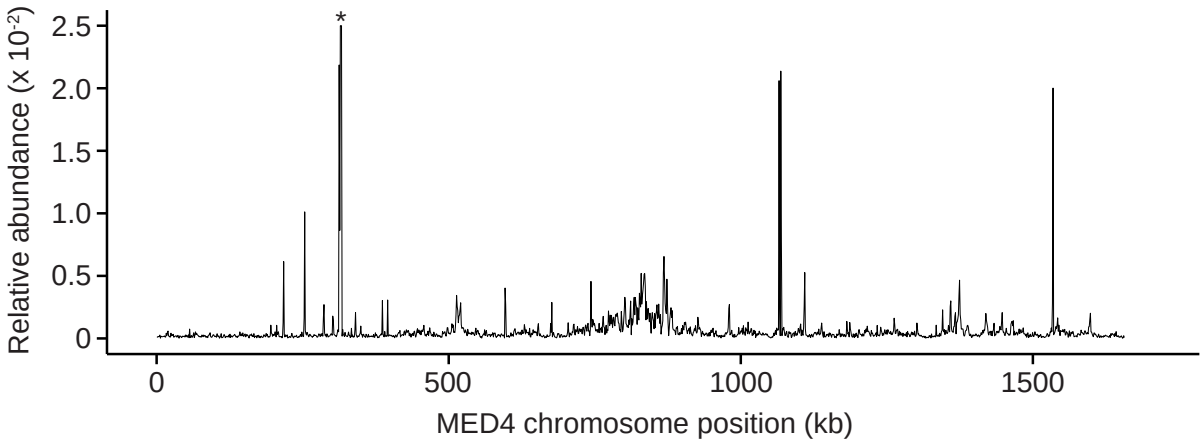

Fig. S8. RNA is associated with *Prochlorococcus* MED4 vesicles. Distribution of RNA associated with vesicles isolated from *Prochlorococcus* MED4 cultures. Sequenced reads were mapped against the MED4 chromosome; mean relative abundance from two replicate samples is plotted over a 1kb window. Due to the use of both rRNA-depleted and non-depleted libraries, relative transcript abundance was calculated excluding ribosomal sequences; a qualitative ribosomal abundance point is plotted for location reference (~310 kb, indicated with *; ribosomal RNA was >94% of all reads in the non-depleted sample). In total, 89% of the genome (1,476,104 bp of the 1,657,990 bp chromosome) was represented at least once in the RNA libraries.

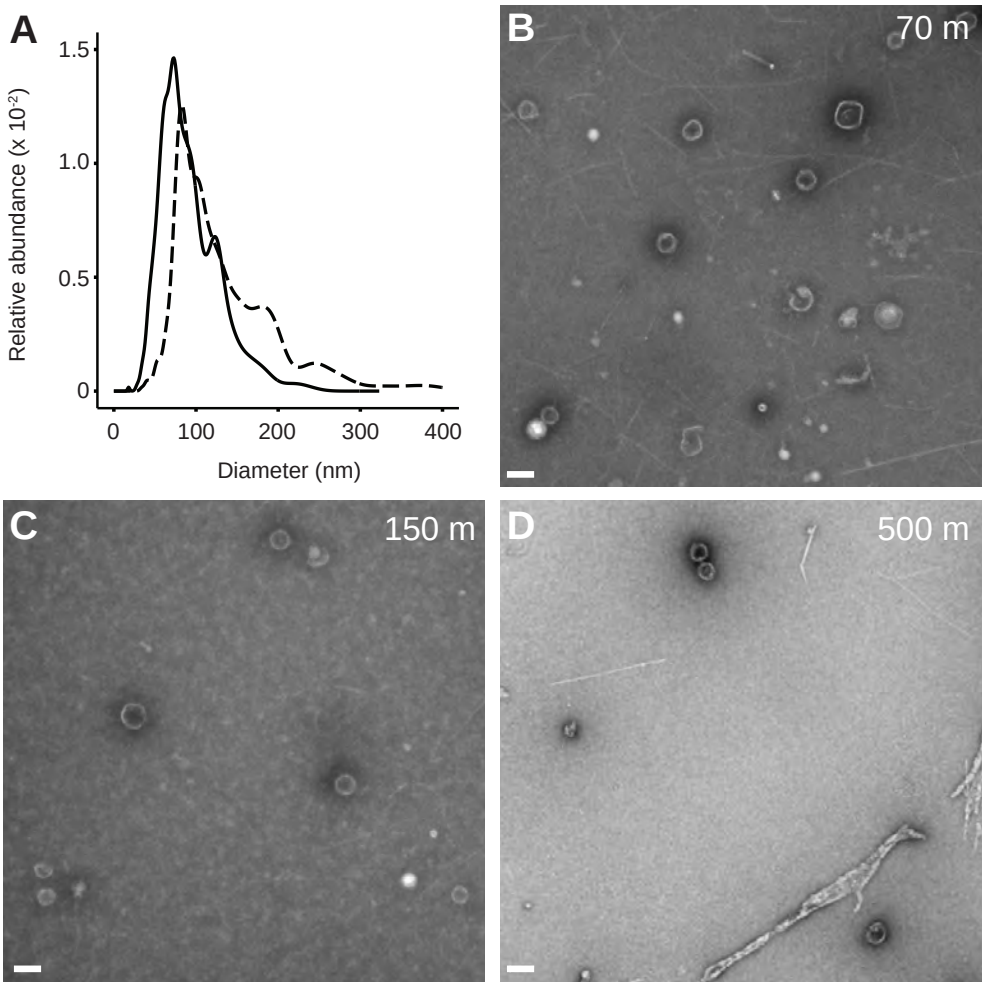

Fig. S9. Bacterial vesicles from the ocean. (**A**) Comparison of vesicle size distributions from 5m depth at the Bermuda Atlantic Time-series Study (BATS) station in the Sargasso Sea (solid line) to coastal surface water from Vineyard Sound, MA (dashed line). (**B-D**) Negatively stained electron micrographs of vesicles from 70m (B), 150m **(**C**)**, and 500m (D) depth at BATS. Scale bars: 100 nm in all panels.

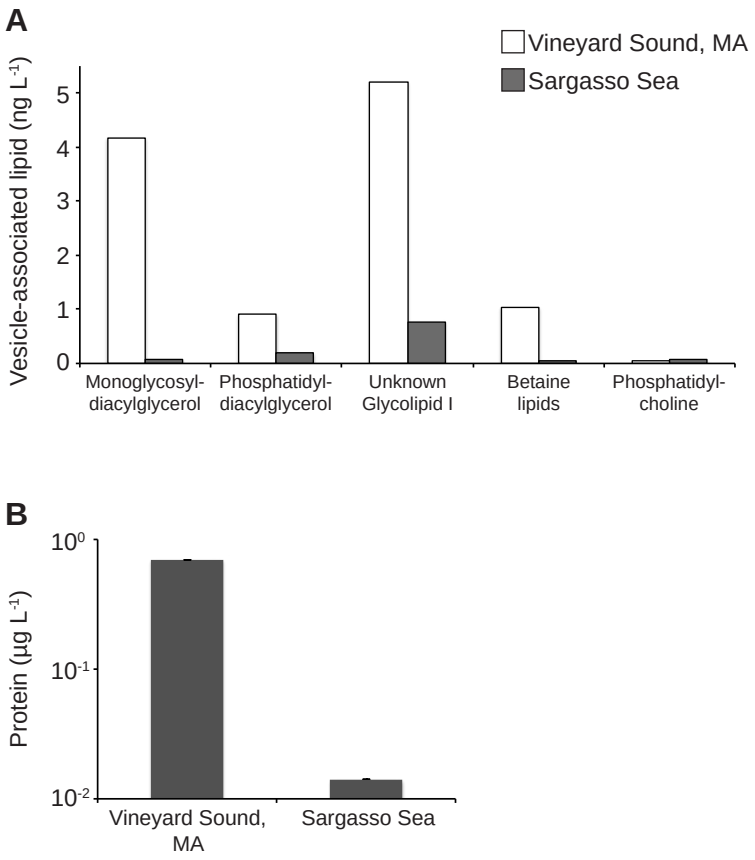

Fig. S10. Vesicle enrichments from ocean samples contain lipid and protein. (**A**) Intact polar lipid headgroup analysis of enriched vesicle samples from the surface of Vineyard Sound, MA (white) and from 5m depth in the Sargasso Sea (grey). Lipid concentrations are normalized to the amount of seawater processed to obtain *in situ* estimates of vesicle-associated lipid concentration. (**B**) Vesicle-associated protein concentrations from the enriched vesicle samples in (A). Protein concentrations, as determined by the BCA assay, are normalized to the amount of seawater processed to obtain *in situ* estimates. Values represent the mean of two replicates.

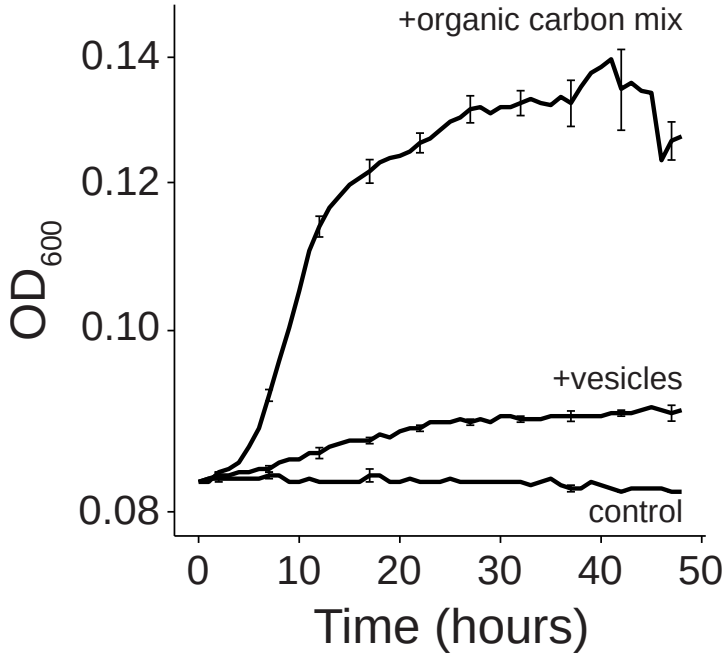

Fig. S11. Heterotrophic utilization of fixed carbon from purified *Prochlorococcus* vesicles. *Halomonas* growth patterns are shown in a seawater-based minimal medium supplemented with media only (control), vesicles (+vesicles), or a defined mixture of organic carbon compounds (+organic carbon mix) as the only added organic carbon source. Growth curves represent the mean +/- SEM of three replicates. The OD_{600} increase of the '+vesicles' and '+organic carbon' trials both corresponded with a significant increase in *Halomonas* cell concentration (measured by plate counts) as compared to the control after 48 hours (*t* test; $p < 0.05$).

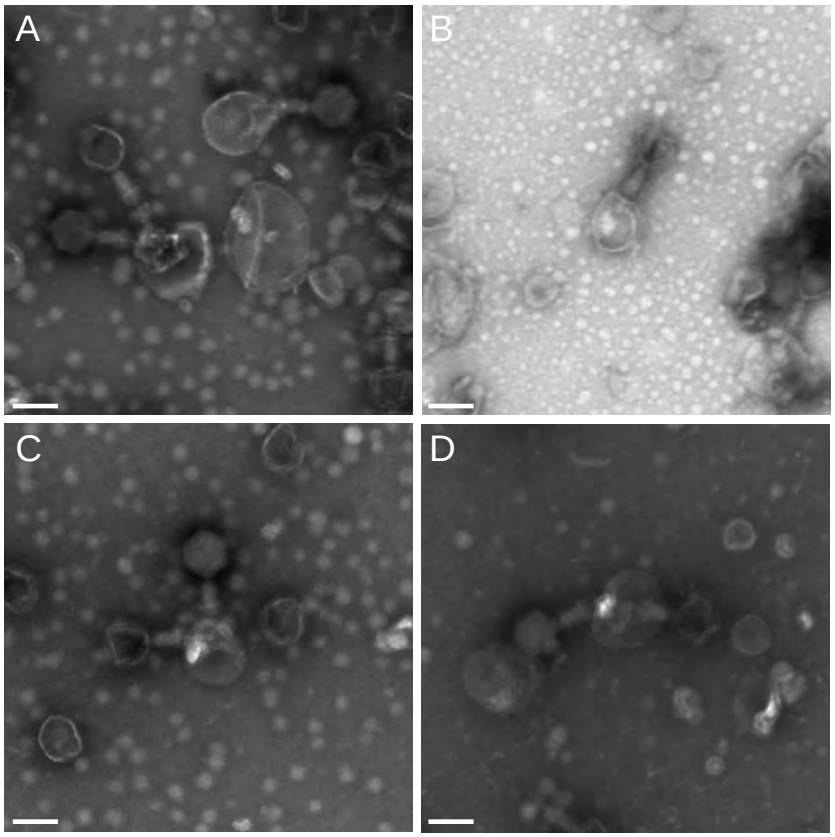

Fig. S12. Additional examples of phage binding to vesicles. (**A-D**) Negatively stained electron micrographs of phage PHM-2 bound to vesicles from *Prochlorococcus* MED4. Scale bar: 100 nm in all frames.

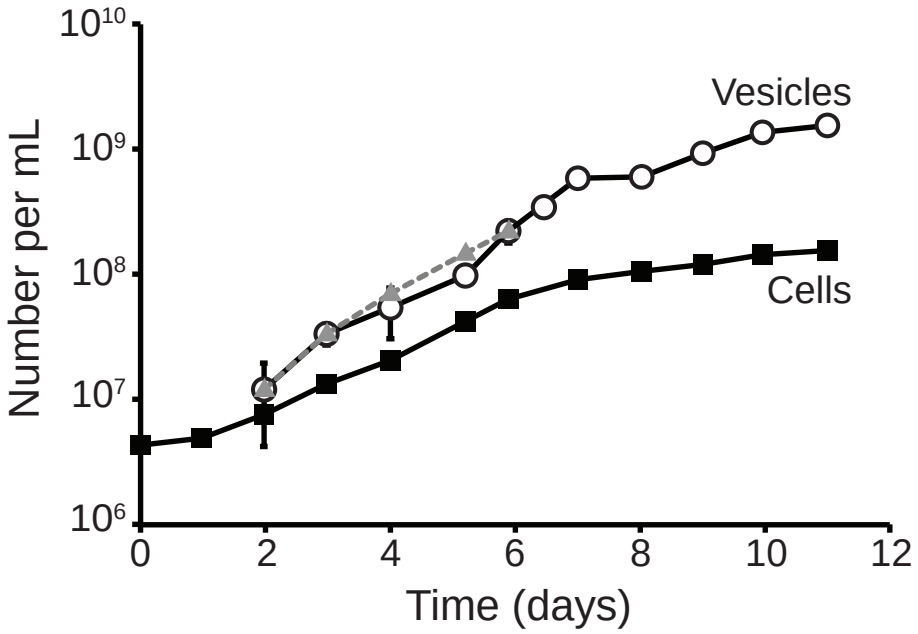

Fig. S13. Fit of vesicle production model to observed data for strain MIT9313. Modeled vesicle production (grey dashed line, triangles) is shown compared to the measured concentration of vesicles (open circles) and cells (squares) in the culture during exponential growth. Modeled values were derived using Eq. 6 (supplementary text), yielding an estimated vesicle production rate r = 3.8 vesicles cell^{-1} generation^{-1}. Modeled and observed values had a correlation coefficient of 0.96.

Table S1. Diverse *Prochlorococcus* strains release membrane vesicles. Axenic *Prochlorococcus* strains found to release vesicle-sized particles in culture. The mode vesicle diameter is based on nanoparticle tracking analysis results of the <0.2 μm culture fraction. nd = not determined.

Strain	Isolation Location	Ecotype group	Mode vesicle diameter (+/- SD), nm	Estimated vesicle production rate (vesicles cell^{-1} generation^{-1})
MED4	Mediterranean Sea	High Light I	91 (± 34)	2.3
MIT9202	Tropical Pacific	High Light II	74 (± 52)	nd
SB	Western Pacific	High Light II	119 (± 97)	nd
MIT9301	Sargasso Sea	High Light II	80 (± 43)	nd
NATL2A	North Atlantic	Low Light I	96 (± 49)	4.7
MIT9313	Gulf Stream	Low Light IV	89 (± 37)	3.8

Table S2. Proteins identified in *Prochlorococcus* MED4 vesicles.

NCBI Accession	Description	Molecular weight (Da)	Mascot identification probability	Predicted localization
gi|33860650|ref|NP_892211.1|	serine protease	41,841.40	100.0%	Periplasmic
gi|33860657|ref|NP_892218.1|	RND family outer membrane efflux protein	54,271.50	100.0%	Outer Membrane
gi|33860667|ref|NP_892228.1|	shikimate kinase	21,235.20	98.1%	Cytoplasmic
gi|33860686|ref|NP_892247.1|	hypothetical protein	36,882.90	100.0%	Cytoplasmic
gi|33860730|ref|NP_892291.1|	NifS-like aminotransferase class-V	42,189.30	99.6%	Cytoplasmic
gi|33860745|ref|NP_892306.1|	hypothetical protein	27,110.60	100.0%	Unknown
gi|33860785|ref|NP_892346.1|	cell division protein FtsH2	66,746.50	99.3%	Cytoplasmic Membrane
gi|33860812|ref|NP_892373.1|	hypothetical protein	77,661.80	100.0%	Outer Membrane
gi|33860888|ref|NP_892449.1|	LysM domain-containing protein	29,279.50	99.6%	Cytoplasmic
gi|33861107|ref|NP_892668.1|	ribulose bisophosphate carboxylase	52,574.50	100.0%	Cytoplasmic
gi|33861234|ref|NP_892795.1|	carboxyl-terminal processing protease	47,966.10	100.0%	Cytoplasmic Membrane
gi|33861267|ref|NP_892828.1|	ABC transporter, substrate binding protein, phosphate	33,888.20	99.8%	Periplasmic
gi|33861350|ref|NP_892911.1|	hypothetical protein PMM0793	44,284.90	97.7%	Cytoplasmic
gi|33861442|ref|NP_893003.1|	D-Ala-D-Ala carboxypeptidase 3	37,303.90	99.8%	Periplasmic
gi|33861470|ref|NP_893031.1|	ABC transporter	43,597.70	99.4%	Cytoplasmic Membrane
gi|33861526|ref|NP_893087.1|	urea ABC transporter, substrate binding protein	47,601.20	98.6%	Cytoplasmic
gi|33861535|ref|NP_893096.1|	hypothetical protein PMM0979	11,172.20	99.9%	Unknown
gi|33861588|ref|NP_893149.1|	ABC transporter substrate-binding protein	52,262.30	99.8%	Unknown
gi|33861680|ref|NP_893241.1|	natural resistance-associated macroph	53,063.10	100.0%	Outer Membrane
gi|33861695|ref|NP_893256.1|	membrane fusion protein	39,592.80	99.8%	Cytoplasmic Membrane
gi|33861718|ref|NP_893279.1|	hypothetical protein	68,499.40	100.0%	Outer Membrane
gi|33861720|ref|NP_893281.1|	iron ABC transporter, substrate binding protein	38,211.60	99.4%	Unknown
gi|33861738|ref|NP_893299.1|	hypothetical protein	22,217.80	100.0%	Unknown
gi|33861749|ref|NP_893310.1|	tetrapyrrole methylase family protein	31,921.30	99.0%	Unknown
gi|33861780|ref|NP_893341.1|	polysaccharide export protein	39,139.10	99.8%	Unknown
gi|33861781|ref|NP_893342.1|	hypothetical protein	68,295.00	99.9%	Unknown
gi|33861795|ref|NP_893356.1|	ABC transporter	67,454.60	99.3%	Cytoplasmic Membrane
gi|33861803|ref|NP_893364.1|	hypothetical protein	46,457.50	100.0%	Cytoplasmic
gi|33861837|ref|NP_893398.1|	GTP-binding protein Era	33,887.90	97.6%	Cytoplasmic Membrane
gi|33861894|ref|NP_893455.1|	chloroplast outer envelope membrane protein	78,853.70	100.0%	Outer Membrane
gi|33861904|ref|NP_893465.1|	sporulation protein SpoIID-like	45,240.70	100.0%	Unknown
gi|33861981|ref|NP_893542.1|	serine protease	49,042.10	100.0%	Periplasmic
gi|33861992|ref|NP_893553.1|	molecular chaperone GroEL	57,442.20	100.0%	Cytoplasmic
gi|33862007|ref|NP_893568.1|	ATP synthase F0F1 subunit alpha	54,341.20	98.3%	Cytoplasmic
gi|33862088|ref|NP_893649.1|	50S ribosomal protein L13	16,112.90	99.8%	Cytoplasmic
gi|33862110|ref|NP_893671.1|	30S ribosomal protein S19	10,192.30	98.5%	Cytoplasmic
gi|33862114|ref|NP_893675.1|	50S ribosomal protein L3	23,168.50	98.8%	Cytoplasmic
gi|33862218|ref|NP_893779.1|	50S ribosomal protein L20	13,478.80	99.8%	Cytoplasmic
gi|33862249|ref|NP_893810.1|	aminotransferase class-IV	32,181.00	99.2%	Cytoplasmic
gi|33862270|ref|NP_893831.1|	hypothetical protein	70,284.00	99.9%	Cytoplasmic Membrane

Table S3. Proteins identified in *Prochlorococcus* MIT9313 vesicles.

NCBI Accession	Description	Molecular weight (Da)	Mascot identification probability	Predicted localization
gi|33862463|ref|NP_894023.1|	LysM domain-containing protein	51,020.80	97.7%	Unknown
gi|33862536|ref|NP_894096.1|	Possible pilin	17,169.30	99.8%	Extracellular
gi|33862667|ref|NP_894227.1|	Cell wall hydrolase/autolysin	38,871.40	99.9%	Unknown
gi|33862915|ref|NP_894475.1|	Hypothetical protein	28,722.20	100.0%	Outer Membrane
gi|33863048|ref|NP_894608.1|	Carboxyl-terminal processing protease	48,733.70	88.0%	Unknown
gi|33863264|ref|NP_894824.1|	ABC transporter, substrate binding protein, phosphate	34,297.40	89.0%	Periplasmic
gi|33863364|ref|NP_894924.1|	Hypothetical protein	18,740.90	99.8%	Unknown
gi|33863369|ref|NP_894929.1|	Possible cAMP phosphodiesterase class-II	14,691.40	99.8%	Unknown
gi|33863565|ref|NP_895125.1|	Hypothetical protein	63,849.60	100.0%	Cytoplasmic
gi|33863660|ref|NP_895220.1|	Hypothetical protein	18,329.30	87.2%	Cytoplasmic
gi|33863680|ref|NP_895240.1|	Chloroplast outer envelope membrane protein homolog	82,961.20	100.0%	Outer Membrane
gi|33863780|ref|NP_895340.1|	Hypothetical protein	35,923.60	87.6%	Outer Membrane
gi|33863782|ref|NP_895342.1|	Sulfatase	87,437.90	98.4%	Unknown
gi|33863784|ref|NP_895344.1|	Possible ABC transporter, solute binding protein	31,284.70	98.6%	Periplasmic
gi|33863788|ref|NP_895348.1|	Hypothetical protein	56,269.20	99.3%	Unknown
gi|33863790|ref|NP_895350.1|	Hypothetical protein	17,057.00	89.0%	Unknown
gi|33863866|ref|NP_895426.1|	Putative magnesium chelatase family protein	11,035.60	89.0%	Cytoplasmic
gi|33863867|ref|NP_895427.1|	Hypothetical protein	25,709.40	100.0%	Unknown
gi|33863886|ref|NP_895446.1|	Possible protein phosphatase 2C	25,307.40	100.0%	Extracellular
gi|33863903|ref|NP_895463.1|	Possible serine protease	40,509.30	100.0%	Periplasmic
gi|33864108|ref|NP_895668.1|	Hypothetical protein	114,133.80	99.8%	Unknown
gi|33864141|ref|NP_895701.1|	Hypothetical protein	25,745.70	100.0%	Unknown
gi|33864244|ref|NP_895804.1|	Possible porin	62,197.20	100.0%	Extracellular
gi|33864366|ref|NP_895926.1|	Hypothetical protein	26,487.30	99.8%	Unknown
gi|33864411|ref|NP_895971.1|	Hypothetical protein	28,534.40	99.8%	Unknown
gi|33864417|ref|NP_895977.1|	Hypothetical protein	80,122.50	99.9%	Unknown
gi|33864493|ref|NP_896053.1|	Putative urea ABC transporter, substrate binding protein	47,029.60	89.0%	Unknown

Table S4. Genes found encoded within *Prochlorococcus* MED4 vesicles. The fifty open reading frames with the highest average read coverage, across the entire gene, are listed below. In total, 1079 open reading frames (out of 1949 total) had an average coverage of at least 1 read from the combined dataset comprising both biological replicate libraries.

Genbank Protein ID	Start	Stop	Description	Average # of reads
158987150	816334	816450	Conserved hypothetical protein	14435
158987183	968405	968758	Conserved hypothetical protein	12615
33634003	825859	826080	30S Ribosomal protein S18	10732
33634004	826089	826283	50S Ribosomal protein L33	9823
33634009	831846	832238	Uncharacterized protein conserved in bacteria	7329
33634011	832609	836169	putative methionine synthase	7034
33633907	736999	737385	hypothetical protein	6351
33634010	832347	832568	conserved hypothetical	5863
33634002	824635	825819	probable ribonuclease II	4461
33639783	467424	468011	putative inorganic pyrophosphatase	4383
33633970	793199	793729	conserved hypothetical protein	3754
33639784	468018	468968	Porphobilinogen deaminase	3700
33634008	830958	831788	possible ATP adenylyltransferase	3662
33633992	815709	816077	hypothetical	3458
158987152	817042	817191	Conserved hypothetical protein	3441
33634005	826385	828850	Phenylalanyl-tRNA synthetase beta chain	3351
33633971	793731	794351	conserved hypothetical protein	3178
33634068	893891	894244	conserved hypothetical protein	3155
33634069	894265	894678	Uncharacterized conserved protein	2962
33634104	927969	929123	putative urea ABC transporter	2903
33634001	823040	824575	Methionyl-tRNA synthetase	2832
33634107	931010	931720	Putative ATP-binding subunit of urea ABC transport system	2832
158987158	915907	916041	Conserved hypothetical protein	2803
33634090	915626	915904	possible GRAM domain	2657
33633993	816587	816823	hypothetical	2656
158987159	916071	916208	Conserved hypothetical protein	2585
33634089	914736	915536	Bacitracin resistance protein BacA	2490
158987160	931750	931929	Conserved hypothetical protein	2485
33634105	929123	930259	putative membrane protein of urea ABC transport system	2274
33634091	916287	916514	conserved hypothetical	2210
33639977	656275	656592	possible Elongation factor Tu domain 2	2171
33634007	829621	830634	possible DnaJ domain	2143
33634106	930252	931007	putative ATP binding subunit of urea ABC transport system	2132
33634088	913686	914414	Peptide methionine sulfoxide reductase	2132
158987151	816447	816587	Conserved hypothetical protein	2117
33633663	156307	157452	Citrate synthase	2108
33633887	713478	714182	30S ribosomal protein S2	2102
33639785	469063	470253	Putative principal RNA polymerase sigma factor	2021
33634067	893041	893874	putative rRNA (adenine-N6,N6)-dimethyltransferase	1977
33639772	456638	457939	glutamate-1-semialdehyde 2,1-aminomutase	1968
33639809	491753	492886	NAD binding site	1955
158987148	815085	815243	Conserved hypothetical protein	1953
33634369	1523605	1524069	conserved hypothetical protein	1941
33634066	892101	893039	Putative 4-diphosphocytidyl-2C-methyl-D-erythritol kinase (CMK)	1939
33634367	1522121	1522831	phycoerythrobilin:ferredoxin oxidoreductase	1915
33639808	490726	491727	Transaldolase	1913
33633960	782376	782627	hypothetical	1854
33634028	857094	857531	Cyclophilin-type peptidyl-prolyl cis-trans isomerase	1813
158987149	815484	815636	Conserved hypothetical protein	1791
158987147	814929	815084	Conserved hypothetical protein	1755

Table S5. Taxonomic distribution of DNA sequences from vesicles. DNA was isolated from vesicles in surface water from coastal (Vineyard Sound, MA) and open ocean (Sargasso Sea) sites, and amplified by multiple displacement amplification prior to library construction. The number of unique best hits to the NCBI nr database, assigned to a given taxonomic group, is reported for all phyla with at least two representative sequences in our data (see additional data table S6 for the detailed identities of all significant hits). Numbers in parentheses indicate the class-level breakdown of sequences assigned to the *Proteobacteria*. See also supplementary online text for a discussion of the viral sequence content.

		Unique database hits	
Superkingdom	**Phylum/Subcategory**	**Coastal**	**Open ocean**
Archaea	*Euryarchaeota*	28	
	Crenarchaeota	6	
Bacteria	*Proteobacteria*	959	201
	Alphaproteobacteria	(56)	(111)
	Betaproteobacteria	(91)	(6)
	Deltaproteobacteria	(21)	(1)
	Epsilonproteobacteria	(18)	(3)
	Gammaproteobacteria	(773)	(80)
	Cyanobacteria	329	176
	Bacteroidetes	317	55
	Firmicutes	215	29
	Actinobacteria	30	6
	Fusobacteria	9	
	Chloroflexi	8	
	Deinococcus-Thermus	7	
	Spirochaetes	7	
	Verrucomicrobia	6	
	Aquificae	5	
	Planctomycetes	5	2
	Chlorobi	3	
	Synergistetes	3	
	Acidobacteria	2	
	Chlamydiae	2	2
	Deferribacteres	2	
	Nitrospirae	2	
Eukaryota	*Streptophyta*	45	8
	Ascomycota	44	11
	Chordata	40	20
	Chlorophyta	18	7
	Basidiomycota	15	3
	Arthropoda	14	5
	Nematoda	12	5
	Apicomplexa	10	3
	Cnidaria	3	
	Platyhelminthes	3	3
	Phaeophyceae	2	
	Placozoa	2	
	Annelida		2
Viral	ssDNA phage (*Circoviridae, Geminiviridae, Microviridae, Nanoviridae*)	359	76
	Unclassified/other	320	96
	Caudovirales (tailed phage)	42	2

References and Notes

1. B. L. Deatherage, B. T. Cookson, Membrane vesicle release in bacteria, eukaryotes, and archaea: A conserved yet underappreciated aspect of microbial life. *Infect. Immun.* **80**, 1948–1957 (2012).

2. A. Kulp, M. J. Kuehn, Biological functions and biogenesis of secreted bacterial outer membrane vesicles. *Annu. Rev. Microbiol.* **64**, 163–184 (2010).

3. J. W. Schertzer, M. Whiteley, A bilayer-couple model of bacterial outer membrane vesicle biogenesis. *MBio* **3**, e00297–e00311 (2012).

4. I. A. MacDonald, M. J. Kuehn, Stress-induced outer membrane vesicle production by *Pseudomonas aeruginosa*. *J. Bacteriol.* **195**, 2971–2981 (2013).

5. J. L. Kadurugamuwa, T. J. Beveridge, Virulence factors are released from *Pseudomonas aeruginosa* in association with membrane vesicles during normal growth and exposure to gentamicin: A novel mechanism of enzyme secretion. *J. Bacteriol.* **177**, 3998–4008 (1995).

6. J. Rivera, R. J. Cordero, A. S. Nakouzi, S. Frases, A. Nicola, A. Casadevall, *Bacillus anthracis* produces membrane-derived vesicles containing biologically active toxins. *Proc. Natl. Acad. Sci. U.S.A.* **107**, 19002–19007 (2010).

7. L. M. Mashburn, M. Whiteley, Membrane vesicles traffic signals and facilitate group activities in a prokaryote. *Nature* **437**, 422–425 (2005).

8. H. Yonezawa, T. Osaki, S. Kurata, M. Fukuda, H. Kawakami, K. Ochiai, T. Hanawa, S. Kamiya, Outer membrane vesicles of *Helicobacter pylori* TK1402 are involved in biofilm formation. *BMC Microbiol.* **9**, 197 (2009).

9. Y. Gorby, J. McLean, A. Korenevsky, K. Rosso, M. Y. El-Naggar, T. J. Beveridge, Redox-reactive membrane vesicles produced by *Shewanella*. *Geobiology* **6**, 232–241 (2008).

10. A. J. Manning, M. J. Kuehn, Contribution of bacterial outer membrane vesicles to innate bacterial defense. *BMC Microbiol.* **11**, 258 (2011).

11. J. A. Roden, D. H. Wells, B. B. Chomel, R. W. Kasten, J. E. Koehler, Hemin binding protein C is found in outer membrane vesicles and protects *Bartonella henselae* against toxic concentrations of hemin. *Infect. Immun.* **80**, 929–942 (2012).

12. G. L. Kolling, K. R. Matthews, Export of virulence genes and Shiga toxin by membrane vesicles of *Escherichia coli* O157:H7. *Appl. Environ. Microbiol.* **65**, 1843–1848 (1999).

13. C. Rumbo, E. Fernández-Moreira, M. Merino, M. Poza, J. A. Mendez, N. C. Soares, A. Mosquera, F. Chaves, G. Bou, Horizontal transfer of the OXA-24 carbapenemase gene via outer membrane vesicles: A new mechanism of dissemination of carbapenem resistance genes in *Acinetobacter baumannii*. *Antimicrob. Agents Chemother.* **55**, 3084–3090 (2011).

14. P. Flombaum, J. L. Gallegos, R. A. Gordillo, J. Rincón, L. L. Zabala, N. Jiao, D. M.

Karl, W. K. Li, M. W. Lomas, D. Veneziano, C. S. Vera, J. A. Vrugt, A. C. Martiny, Present and future global distributions of the marine Cyanobacteria *Prochlorococcus* and *Synechococcus*. *Proc. Natl. Acad. Sci. U.S.A.* **110**, 9824–9829 (2013).

15. F. Partensky, L. Garczarek, *Prochlorococcus*: advantages and limits of minimalism. *Annu. Rev. Mar. Sci.* **2**, 305–331 (2010).

16. Materials and methods are available as supplementary material on *Science* on the Web.

17. D. Mug-Opstelten, B. Witholt, Preferential release of new outer membrane fragments by exponentially growing *Escherichia coli*. *Biochim. Biophys. Acta* **508**, 287–295 (1978).

18. B. A. S. Van Mooy, G. Rocap, H. F. Fredricks, C. T. Evans, A. H. Devol, Sulfolipids dramatically decrease phosphorus demand by picocyanobacteria in oligotrophic marine environments. *Proc. Natl. Acad. Sci. U.S.A.* **103**, 8607–8612 (2006).

19. N. Borch, D. Kirchman, Protection of protein from bacterial degradation by submicron particles. *Aquat. Microb. Ecol.* **16**, 265–272 (1999).

20. E. Tanoue, S. Nishiyama, M. Kamo, A. Tsugita, Bacterial membranes: Possible source of a major dissolved protein in seawater. *Geochim. Cosmochim. Acta* **59**, 2643–2648 (1995).

21. H. X. Chiura, K. Kogure, S. Hagemann, A. Ellinger, B. Velimirov, Evidence for particle-induced horizontal gene transfer and serial transduction between bacteria. *FEMS Microbiol. Ecol.* **76**, 576–591 (2011).

22. S. Bertilsson, O. Berglund, M. Pullin, S. Chisholm, Release of dissolved organic matter by *Prochlorococcus*. *Vie Milieu* **55**, 225–232 (2005).

23. L. Aluwihare, D. Repeta, R. Chen, A major biopolymeric component to dissolved organic carbon in surface sea water. *Nature* **387**, 166–169 (1997).

24. A. Shibata, K. Kogure, I. Koike, K. Ohwada, Formation of submicron colloidal particles from marine bacteria by viral infection. *Mar. Ecol. Prog. Ser.* **155**, 303–307 (1997).

25. J. J. Grzymski, A. M. Dussaq, The significance of nitrogen cost minimization in proteomes of marine microorganisms. *ISME J.* **6**, 71–80 (2012).

26. D. Sher, J. W. Thompson, N. Kashtan, L. Croal, S. W. Chisholm, Response of *Prochlorococcus* ecotypes to co-culture with diverse marine bacteria. *ISME J.* **5**, 1125–1132 (2011).

27. J. J. Morris, Z. I. Johnson, M. J. Szul, M. Keller, E. R. Zinser, Dependence of the cyanobacterium *Prochlorococcus* on hydrogen peroxide scavenging microbes for growth at the ocean's surface. *PLoS ONE* **6**, e16805 (2011).

28. R. J. Parsons, M. Breitbart, M. W. Lomas, C. A. Carlson, Ocean time-series reveals recurring seasonal patterns of virioplankton dynamics in the northwestern Sargasso Sea. *ISME J.* **6**, 273–284 (2012).

29. A. V. Klieve, M. T. Yokoyama, R. J. Forster, D. Ouwerkerk, P. A. Bain, E. L. Mawhinney, Naturally occurring DNA transfer system associated with membrane vesicles in cellulolytic *Ruminococcus* spp. of ruminal origin. *Appl. Environ. Microbiol.* **71**, 4248–4253 (2005).

30. M. L. Wells, E. D. Goldberg, Occurrence of small colloids in sea water. *Nature* **353**, 342–344 (1991).

31. L. Moore, A. Coe, E. R. Zinser, M. A. Saito, M. B. Sullivan, D. Lindell, K. Frois-Moniz, J. Waterbury, S. W. Chisholm, Culturing the marine cyanobacterium *Prochlorococcus*. *Limnol. Oceanogr. Methods* **5**, 353–362 (2007).

32. A. L. Horstman, M. J. Kuehn, Enterotoxigenic *Escherichia coli* secretes active heat-labile enterotoxin via outer membrane vesicles. *J. Biol. Chem.* **275**, 12489–12496 (2000).

33. H. F. Sturt, R. E. Summons, K. Smith, M. Elvert, K.-U. Hinrichs, Intact polar membrane lipids in prokaryotes and sediments deciphered by high-performance liquid chromatography/electrospray ionization multistage mass spectrometry—new biomarkers for biogeochemistry and microbial ecology. *Rapid Commun. Mass Spectrom.* **18**, 617–628 (2004).

34. L. Wörmer, J. S. Lipp, J. M. Schröder, K.-U. Hinrichs, Application of two new LC-ESI-MS methods for improved detection of intact polar lipids (IPLs) in environmental samples. *Org. Geochem.* **59**, 10–21 (2013).

35. N. Y. Yu, J. R. Wagner, M. R. Laird, G. Melli, S. Rey, R. Lo, P. Dao, S. C. Sahinalp, M. Ester, L. J. Foster, F. S. Brinkman, PSORTb 3.0: Improved protein subcellular localization prediction with refined localization subcategories and predictive capabilities for all prokaryotes. *Bioinformatics* **26**, 1608–1615 (2010).

36. M. Renelli, V. Matias, R. Y. Lo, T. J. Beveridge, DNA-containing membrane vesicles of *Pseudomonas aeruginosa* PAO1 and their genetic transformation potential. *Microbiology* **150**, 2161–2169 (2004).

37. G. Giannoukos, D. M. Ciulla, K. Huang, B. J. Haas, J. Izard, J. Z. Levin, J. Livny, A. M. Earl, D. Gevers, D. V. Ward, C. Nusbaum, B. W. Birren, A. Gnirke, Efficient and robust RNA-seq process for cultured bacteria and complex community transcriptomes. *Genome Biol.* **13**, r23 (2012).

38. T. Woyke, A. Sczyrba, J. Lee, C. Rinke, D. Tighe, S. Clingenpeel, R. Malmstrom, R. Stepanauskas, J. F. Cheng, Decontamination of MDA reagents for single cell whole genome amplification. *PLoS ONE* **6**, e26161 (2011).

39. S. Rodrigue, R. R. Malmstrom, A. M. Berlin, B. W. Birren, M. R. Henn, S. W. Chisholm, Whole genome amplification and de novo assembly of single bacterial cells. *PLoS ONE* **4**, e6864 (2009).

40. H. Li, R. Durbin, Fast and accurate short read alignment with Burrows-Wheeler transform. *Bioinformatics* **25**, 1754–1760 (2009).

41. H. Li, B. Handsaker, A. Wysoker, T. Fennell, J. Ruan, N. Homer, G. Marth, G. Abecasis, R. Durbin; 1000 Genome Project Data Processing Subgroup, The

Sequence Alignment/Map format and SAMtools. *Bioinformatics* **25**, 2078–2079 (2009).

42. S. Rodrigue, A. C. Materna, S. C. Timberlake, M. C. Blackburn, R. R. Malmstrom, E. J. Alm, S. W. Chisholm, Unlocking short read sequencing for metagenomics. *PLoS ONE* **5**, e11840 (2010).

43. R. C. Edgar, UBLAST algorithm (v6.0.307), http://drive5.com/usearch.

44. K.-H. Kim, J.-W. Bae, Amplification methods bias metagenomic libraries of uncultured single-stranded and double-stranded DNA viruses. *Appl. Environ. Microbiol.* **77**, 7663–7668 (2011).

45. J. J. Morris, R. Kirkegaard, M. J. Szul, Z. I. Johnson, E. R. Zinser, Facilitation of robust growth of *Prochlorococcus* colonies and dilute liquid cultures by "helper" heterotrophic bacteria. *Appl. Environ. Microbiol.* **74**, 4530–4534 (2008).

46. J. J. López Cascales, J. García de la Torre, S. J. Marrink, H. J. C. Berendsen, Molecular dynamics simulation of a charged biological membrane. *J. Chem. Phys.* **104**, 2713–2720 (1996).

47. H. Nikaido, in Escherichia coli and Salmonella typhimurium: Cellular and Molecular Biology, F. C. Neidhardt, Ed. (ASM Press, 1996).

48. R. Fukuda, H. Ogawa, T. Nagata, I. Koike, Direct determination of carbon and nitrogen contents of natural bacterial assemblages in marine environments. *Appl. Environ. Microbiol.* **64**, 3352–3358 (1998).

49. D. Vaulot, D. Marie, R. J. Olson, S. W. Chisholm, Growth of prochlorococcus, a photosynthetic prokaryote, in the equatorial pacific ocean. *Science* **268**, 1480–1482 (1995).

50. E. L. Mann, S. W. Chisholm, Iron limits the cell division rate of Prochlorococcus in the eastern equatorial Pacific. *Limnol. Oceanogr.* **45**, 1067–1076 (2000).

51. H. Wada, N. Murata, in *Lipids in Photosynthesis: Structure, Function and Genetics*, P. A. Siegenthaler, N. Murata, Eds. (Kluwer Academic Publishers, 1998), pp. 65–81.

52. M. T. Brett, D. C. Muller-Navarra, The role of highly unsaturated fatty acids in aquatic foodweb processes. *Freshw. Biol.* **38**, 483–499 (1997).

53. C. Sohlenkamp, I. M. López-Lara, O. Geiger, Biosynthesis of phosphatidylcholine in bacteria. *Prog. Lipid Res.* **42**, 115–162 (2003).

54. O. Geiger, N. González-Silva, I. M. López-Lara, C. Sohlenkamp, Amino acid-containing membrane lipids in bacteria. *Prog. Lipid Res.* **49**, 46–60 (2010).

55. V. P. Edgcomb, J. M. Bernhard, D. Beaudoin, S. Pruss, P. V. Welander, F. Schubotz, S. Mehay, A. L. Gillespie, R. E. Summons, Molecular indicators of microbial diversity in oolitic sands of Highborne Cay, Bahamas. *Geobiology* **11**, 234–251 (2013).

56. K. J. Popendorf, M. W. Lomas, B. A. S. Van Mooy, Microbial sources of intact polar diacylglycerolipids in the Western North Atlantic Ocean. *Org. Geochem.* **42**, 803–811 (2011).

57. D. Lindell, M. B. Sullivan, Z. I. Johnson, A. C. Tolonen, F. Rohwer, S. W. Chisholm, Transfer of photosynthesis genes to and from *Prochlorococcus* viruses. *Proc. Natl. Acad. Sci. U.S.A.* **101**, 11013–11018 (2004).

58. N. H. Mann, M. R. Clokie, A. Millard, A. Cook, W. H. Wilson, P. J. Wheatley, A. Letarov, H. M. Krisch, The genome of S-PM2, a "photosynthetic" T4-type bacteriophage that infects marine *Synechococcus* strains. *J. Bacteriol.* **187**, 3188–3200 (2005).

59. M. B. Sullivan, M. L. Coleman, P. Weigele, F. Rohwer, S. W. Chisholm, Three *Prochlorococcus* cyanophage genomes: Signature features and ecological interpretations. *PLoS Biol.* **3**, e144 (2005).

60. P. R. Weigele, W. H. Pope, M. L. Pedulla, J. M. Houtz, A. L. Smith, J. F. Conway, J. King, G. F. Hatfull, J. G. Lawrence, R. W. Hendrix, Genomic and structural analysis of Syn9, a cyanophage infecting marine *Prochlorococcus* and *Synechococcus*. *Environ. Microbiol.* **9**, 1675–1695 (2007).

61. M. B. Sullivan, K. H. Huang, J. C. Ignacio-Espinoza, A. M. Berlin, L. Kelly, P. R. Weigele, A. S. DeFrancesco, S. E. Kern, L. R. Thompson, S. Young, C. Yandava, R. Fu, B. Krastins, M. Chase, D. Sarracino, M. S. Osburne, M. R. Henn, S. W. Chisholm, Genomic analysis of oceanic cyanobacterial myoviruses compared with T4-like myoviruses from diverse hosts and environments. *Environ. Microbiol.* **12**, 3035–3056 (2010).

62. K. Holmfeldt, N. Solonenko, M. Shah, K. Corrier, L. Riemann, N. C. Verberkmoes, M. B. Sullivan, Twelve previously unknown phage genera are ubiquitous in global oceans. *Proc. Natl. Acad. Sci. U.S.A.* **110**, 12798–12803 (2013).

63. K. P. Tucker, R. Parsons, E. M. Symonds, M. Breitbart, Diversity and distribution of single-stranded DNA phages in the North Atlantic Ocean. *ISME J.* **5**, 822–830 (2011).